



## 34 1. INTRODUCTION

35 Rapid ecosystem changes in relation to changing environmental conditions have been  
36 reported in a wide variety of ecosystems (e.g. Hoegh-Guldberg et al. 2007, Fossheim et al.  
37 2015, Sahade et al. 2015, Thomson et al. 2015). Changes in environmental conditions may  
38 affect species directly by challenging their physiological tolerance levels or indirectly by  
39 disrupting vital interspecies interactions (Tylianakis et al. 2008). Species may respond with  
40 changes in abundance or shifts in distribution (Florko et al. 2018).

41 The Gulf of St. Lawrence (GSL), Eastern Canada, has seen major and potentially far-reaching  
42 ecosystem changes over the past decades due to climate change and anthropogenic  
43 pressures. In the early 1990s, overfishing culminated in the collapse of Atlantic cod (*Gadus*  
44 *morhua*) and other large demersal fish stocks, marking a fishery-induced regime shift in the  
45 ecosystem (Savenkoff et al. 2007, Bui et al. 2010). Simultaneously, unprecedented warming  
46 of incoming North Atlantic water, changes in sea surface temperature (SST), salinity and sea  
47 ice extent altered the habitat significantly (Thibodeau et al. 2010, Plourde et al. 2014).  
48 Higher mortality rates in response to these ecosystem changes were reported even in higher  
49 predators, such as harp seals (*Pagophilus groenlandicus*) and belugas (*Delphinapterus*  
50 *leucas*), highlighting the cascading effects of the changing environmental conditions  
51 (Johnston et al. 2012, Plourde et al. 2014).

52 In this context, this study aimed to study the spatio-temporal patterns in fin whale  
53 (*Balaenoptera physalus*) distribution and abundance in the northern GSL. Schleimer et al.  
54 (2019) found a significant decline in the number of fin whales using this feeding area and  
55 evidence of declining survival rates over the past decade. However, a shift in distribution (i.e.  
56 permanent emigration) in response to ecosystem changes in the GSL was also proposed as

57 an possible explanation for the decline in numbers. Fin whales in the GSL have been found to  
58 shift arrival dates to the feeding ground in the GSL at a rate of one day earlier per year over  
59 three decades, linked to earlier winter sea ice break up and higher SST (Ramp et al. 2015).  
60 Fin whale distribution has been correlated with the occurrence of thermal fronts in the GSL  
61 (Doniol-Valcroze et al. 2007); however, the physical and biological processes that drive intra-  
62 and inter-annual variation in distribution of fin whales in the GSL remain poorly understood.

63 Here, we hypothesise that the observed changes in abundance could be attributed to  
64 changes in environmental conditions. To test this hypothesis, spatio-temporal patterns in fin  
65 whale distribution were explored within a species distribution model (SDM) framework  
66 (Redfern et al. 2006, Forney et al. 2012, Hazen et al. 2017). SDMs aim to identify the  
67 underlying factors that drive spatio-temporal trends in species' distribution, offering insight  
68 into both the causes of past responses and predictions of future responses to a changing  
69 environment (Hazen et al. 2013, Víkingsson et al. 2015). If changes in the environmental  
70 conditions in the GSL, as reflected by changes in sea temperature, primary productivity or  
71 prey biomass, were at the basis of the observed decline in abundance of fin whales, we  
72 expected to detect such a relationship in the SDMs with the retention of dynamic variables  
73 in the final model. Extensive survey and effort data collected in the northern GSL over seven  
74 summers provided the basis of this study. SDMs frequently use proxy variables that are  
75 assumed to be indicative of high productivity and prey distribution (Torres et al. 2008). Here,  
76 two separate SDMs were built. The first SDM modelled fin whale relative abundance as a  
77 function of commonly used proxy variables for high productivity (including bathymetric and  
78 remotely sensed oceanographic variables), while the second SDM used modelled krill  
79 biomass as explanatory variable in place of the proxy variables used to derive it (Plourde et  
80 al. 2016). Specifically, we wanted to test whether the modelled prey variable would provide

81 better predictive power to a model based on proxy variables to define fin whale habitat.  
82 Euphausiids constitute an important component of fin whale diet in the GSL (Gavrilchuk et  
83 al. 2014) and a strong link between fin whale distribution and euphausiid biomass is  
84 expected. We wanted to test whether euphausiid biomass derived from a model could serve  
85 as informative alternative to high-resolution prey data despite the inherent uncertainty that  
86 is associated with habitat model predictions.

87 Ideally, cetacean-habitat models are built using data derived from systematic surveys  
88 specifically designed to estimate cetacean density and abundance. However, given cost and  
89 scheduling limitations imposed by such dedicated surveys, there is a growing interest in  
90 developing methods to account for the biases associated with non-systematic or  
91 opportunistic surveys (e.g. Williams et al. 2006, Phillips et al. 2009, Isojunno et al. 2012). The  
92 fin whale data used in the present study were collected as part of a photo-identification  
93 study; as such, the survey design differed from conventional systematic cetacean surveys in  
94 three ways; (1) surveys were not designed to ensure equal coverage probability, (2)  
95 distance-sampling was not implemented, and (3) search effort was interrupted by the  
96 collection of sighting-specific data (e.g. photo-identification and biopsy data). The nature of  
97 the data prohibited a design-based approach, necessitating a model-based approach, using  
98 generalised additive models (GAMs), which does not require random placement of survey  
99 lines in the study area. Additionally, the concept of “handling time” was applied to  
100 differentiate between time spent collecting sighting-specific data and search effort. The  
101 proposed methods are applicable to other studies that rely on opportunistically collected  
102 data, such as cetacean data collected during whale watching activities.

## 103 **2. MATERIALS & METHODS**

## 104 **2.1 Cetacean Survey Data**

105 The study area was located in the Jacques Cartier Passage (JCP), between Anticosti Island  
106 and the North Shore in the GSL, extending over an area of approximately 8000 km<sup>2</sup> (Fig. 1).

107 The region covers diverse topographic features, such as the head of the Anticosti Channel,  
108 the steep slopes along Anticosti Island, and the shallower plateaus of the North Shore and  
109 Banc Parent. Upwelling of cold, nutrient rich waters from the cold intermediate layer place  
110 the region among the most productive in the GSL, allowing the ecosystem to sustain a high  
111 biodiversity (Bourque et al. 1995, Doniol-Valcroze et al. 2007). During summer months,  
112 minke whales (*Balaenoptera acutorostrata*), humpback whales (*Megaptera novaeangliae*),  
113 fin whales and harbour porpoises (*Phocoena phocoena*) co-occur in the study area, with  
114 occasional sightings of blue whales (*B. musculus*) and, more recently, North Atlantic right  
115 whales (*Eubalaena glacialis*).

116 Cetacean survey data were collected by researchers from Mingan Island Cetacean Study  
117 from June to October in the years of 2007 to 2013. The data used for the purpose of this  
118 study consisted of the non-random survey tracks and the position, timing, and group size of  
119 each fin whale sighting. Surveys were conducted using rigid-hulled inflatable boats and  
120 focussed on the collection of photo-identification data of large rorquals. The survey design is  
121 therefore best described in terms of “whaler-behaviour” meaning that captains targeted  
122 areas where they expected to find animals to maximise photo-identification effort. The  
123 surveys covered as large an area as possible until groups of whales were found. Boat speed  
124 varied between 15 and 20 knots, with occasional stops to scan the horizon with binoculars  
125 for blows. For safety reasons, two boats conducted surveys simultaneously, but they  
126 generally covered different areas. Surveys were terminated when weather conditions  
127 deteriorated to Beaufort scale >3 or visibility <1nm.

128 Once an individual or group of whales was detected, the time of the sighting was noted and  
129 the animals were approached slowly for collection of photo-identification and sometimes  
130 biopsy data. The exact position was recorded at the 'fluke print' where the animal dived  
131 after its surfacing sequence. The group size of animals was recorded and individuals were  
132 attributed field-ID numbers to keep track of individuals on subsequent sightings. Field-ID  
133 numbers and photo-identification data were used to determine whether individuals had  
134 already been sighted previously. If individuals were not identifiable, the group was  
135 considered to be a new sighting.

## 136 **2.2 Data Processing**

### 137 *2.2.1 Effort Quantification*

138 The survey track was recorded using a LOWRANCE LMS-480M GPS unit (precision  $\leq 30$  m) on  
139 each survey boat. The resulting survey tracks were used to calculate survey effort. Due to  
140 variable boat speeds and *ad libitum* survey tracks, the length of the survey track was not  
141 considered an appropriate measure of effort. Instead effort was defined as the time in  
142 seconds spent searching for animals within a grid cell (see below). Timestamps were  
143 retrieved from the GPS tracks to estimate the effort spent in each grid cell (see  
144 Supplementary Fig. S1).

145 A grid-based modelling framework was adopted in accordance with previous studies dealing  
146 with non-systematic survey designs (Cañadas et al. 2005, Isojunno et al. 2012). The study  
147 area was divided into 5 x 5 km grid cells in which the number of fin whale individuals, effort  
148 and environmental covariates could be summarised. The size of the grid cells was chosen  
149 based primarily on the resolution of available remotely sensed and modelled covariates  
150 (Table 1).

151 While time identified as 'off effort' was excluded from the calculations, the strong focus on  
152 photo-identification and biopsy sampling made further modification of the effort data  
153 necessary. When the researchers were concentrating on obtaining photo-identification data  
154 and taking biopsy samples, all effort was focused on a single individual or group, rather than  
155 searching for new groups. Because the surveys covered all cetacean species encountered,  
156 such interruptions of search effort were not limited to fin whale encounters. Because of  
157 similar bias, Isojunno et al. (2012) did not consider duration of grid cell visits to be an  
158 adequate measure of effort. Here, we corrected the total time spent in each grid cell by  
159 removing effort associated with the collection of sighting-specific data. From the survey data  
160 it was possible to identify sequential re-sightings of the same group during which such data  
161 were taken. The time from the first re-sighting to the last re-sighting of a group was  
162 characterised as "handling time" and considered off effort. A similar approach has been used  
163 to calculate search effort of whalers, where the chasing and processing of caught whales was  
164 considered "handling time" and was excluded from the general search effort (Sigurjónsson  
165 1988, Sigurjónsson & Gunnlaugsson 2006). This approach more accurately reflected time  
166 spent searching for fin whales and allowed us to use time as an offset in our models.

### 167 *2.2.2. Environmental Data*

168 Environmental data were chosen based on 1) their importance in previous cetacean species  
169 distribution models and 2) their availability at a sufficiently fine spatial resolution with  
170 respect to the 25 km<sup>2</sup> grid resolution of the sightings and effort data (Table 1). The data set  
171 was subdivided into months to allow seasonal and inter-annual variation in time-variable  
172 covariates (SST, chlorophyll  $\alpha$ , krill biomass) to be incorporated. Month was chosen as an  
173 appropriate time period to minimise gaps in remotely sensed data, which tend to have  
174 significantly fewer missing data due to cloud cover when summarised per month compared

175 to daily or weekly resolutions. Fin whale sighting and survey effort data were pooled for  
176 each month of the field season, resulting in a maximum of 35 (five months x seven years)  
177 temporal sub-units per grid cell. Greene and Pershing (2000) proposed a conceptual model  
178 linking North Atlantic Oscillation (NAO), physical environmental conditions, and zooplankton  
179 in the northwest Atlantic. This distant potential link was explored in our analyses by  
180 including NAO indices as explanatory variables. Hurrell's PC-based NAO index was used in  
181 this study for monthly and winter NAO indices (Hurrell et al. 2003). Previous studies have  
182 shown that abundance of balaenopterids typically lag behind maximum primary productivity  
183 by several weeks (Croll et al. 2005, Visser et al. 2011, Ramp et al. 2015). The possible effect  
184 of a temporal lag in the response of fin whale distribution to proxy variables was assessed by  
185 including composite spring SST and chlorophyll  $a$  concentrations (Chl  $a$ ) and lagged winter  
186 NAO indices.

187 In the absence of high-resolution euphausiid data covering the entire study area/period, krill  
188 biomass was derived from a krill habitat model as described in Plourde et al. (2016). Briefly,  
189 Plourde et al. (2016) modelled krill biomass spatial and temporal distribution in eastern  
190 Canadian waters as a function of static (bathymetry and slope) and dynamic (SST, Chl  $a$ , sea  
191 level height anomaly) environmental variables in a GAM framework. High-resolution  
192 quantification of euphausiid biomass was available from multifrequency acoustic data  
193 collected from surveys in the GSL (including the JCP) and adjacent waters since 2000  
194 (McQuinn et al. 2015). The final euphausiid biomass model explained 24.5 % of deviance and  
195 was used to get monthly predictions of krill biomass at 5 x 5 km resolution in the JCP for the  
196 present study. Due to the spatial overlap of both studies, no extrapolations beyond the  
197 range of explanatory variables were necessary.

### 198 **2.3. Data Analysis**

199 The relationship between the number of fin whale individuals in each grid cell (response  
200 variable) and the explanatory variables was modelled using GAMs (Hastie & Tibshirani 1990,  
201 Wood 2017), which are commonly used to study spatial and temporal drivers in cetacean  
202 distribution because of their flexibility (Redfern et al. 2006, 2017, Isojunno et al. 2012,  
203 Becker et al. 2016). Only grid cells with search effort were used to build the model. GAMs  
204 were fitted in the R (v. 3.2.3, R Core Team 2015) package *mgcv* (v. 1.8-25; Wood 2017).

205 Two separate models were built to model temporal and spatial patterns in fin whale  
206 distribution. The first model (the proxy model) included all static and dynamic environmental  
207 proxy variables (all variables listed in Table 1, except for krill biomass), including month and  
208 year. The second model (the prey model) included only modelled krill biomass, month and  
209 year, thus excluding the remaining proxy variables (most of which were used in the model to  
210 predict krill biomass). In both models, the number of individual fin whales per grid cell was  
211 modelled as a negative binomial distribution with logarithmic link function. The response  
212 variable was characterised by a high frequency of zeros (3207 grid cells without sightings  
213 compared to 312 grid cells with sightings) and the negative binomial error distribution  
214 provided the best fit to the data (Supplement S2). The negative binomial distribution has  
215 been used in previous studies with similar types of data (i.e. count data with many zeros and  
216 overdispersion; Warton 2005, Virgili et al. 2017). The natural logarithm of monthly search  
217 effort was included as an offset term in the model to account for variable search effort  
218 across the study area. Only the first encounter of a fin whale individual/group was counted  
219 towards the monthly sum of fin whales in each grid cell to avoid the inclusion of duplicate  
220 sightings. Sightings data collected on the same day from different survey boats were treated  
221 independently because the spatial coverage differed between boats.

222 Prior to model fitting, explanatory variables were inspected for collinearity using the pairs  
223 function from the *AED* package in R, which generates a correlation matrix for pair-wise  
224 comparison between variables (Zuur et al. 2009). Two variables were deemed collinear if the  
225 estimated Pearson correlation coefficient exceeded 0.6. No collinearity was detected among  
226 covariates (Supplement 3, Fig. S3). Chl *a* and krill biomass values were log transformed  
227 ( $\log(X + 1)$ ) to reduce skewness in the data. Field observations suggested that fin whales  
228 fed in shallower waters on the North Shore in June and July; interaction terms of month with  
229 depth and with aspect were thus considered to explore whether the data supported these  
230 relationships.

231 Restricted maximum likelihood (REML) was used for smoothing parameter estimation  
232 (Marra & Wood 2011). The gamma term, which acts as an additional penalty, was set to 1.4  
233 to reduce over-fitting in cases with relatively few observations per variable (Kim & Gu 2004,  
234 Wood 2006). Full models with and without interaction terms were fitted with penalised  
235 cubic regression splines and tensor products (*ti*) for interaction terms. A cyclic regression  
236 spline was fitted to aspect (0-360°) to match start and end points. Shrinkage spline smooths  
237 were used for covariate selection. The shrinkage approach penalises the null space of the  
238 smooth function, reducing the degrees of freedom of unsupported covariates to zero,  
239 allowing multiple terms to be dropped from the full model in a single step (Marra & Wood  
240 2011).

241 Models with and without interaction terms were compared using Akaike Information  
242 Criterion (AIC; Akaike 1972, Wood et al. 2016), percentage of deviance explained, and  
243 average squared prediction error (ASPE). To calculate the latter, a five-fold cross-validation  
244 was applied to assess the performance of candidate models in predicting novel data. Data  
245 were randomly split into five subsets. Models were fitted to 80% of the data for model

246 training and the remaining 20% of the data were subsequently used for validation of  
247 predictions based on the trained model. ASPE was calculated as the mean squared  
248 difference between predicted and observed fin whale numbers in the validation subset. This  
249 cross-validation was run five-times in total and the mean ASPE was retained for model  
250 selection.

251 The final chosen model was refitted with the complete data set. If terms with an  
252 approximate  $P$ -value  $>0.05$  remained in the model after shrinkage, the covariate with the  
253 least significant  $P$ -value was dropped from the model. If the exclusion of the variable did not  
254 increase the AIC score, the reduced model was retained. The relative covariate importance  
255 was estimated with the R function *varImpBiomod* (Thuiller et al. 2009). Model residual plots  
256 were examined visually to verify that assumptions of normality and variance homogeneity  
257 were met (Figs. S4 & S5). Spatial autocorrelation of model residuals was assessed using a  
258 variogram (Zuur et al. 2009).

#### 259 **2.4. Prediction**

260 The final proxy and prey models were used to compute predictions of relative abundance  
261 (individuals/hour) in each grid cell. Predictive maps were generated for each year, fixing the  
262 offset term to one hour of effort in each grid cell per month, in the open source GIS software  
263 package Quantum GIS (QGIS v. 2.18.1; QGIS Development Team, 2016). Because the model  
264 yielded separate predictions for each month, the mean relative abundance per year was  
265 plotted. To assess prediction uncertainty, coefficients of variation (CV) were calculated  
266 based on posterior simulation. From the posterior distributions of the model coefficients,  
267 1000 coefficient vectors were simulated using *mvrnorm* from the R MASS library (Venables  
268 and Ripley 2002) and were used to generate 1000 predictions. The mean and CV were

269 calculated from these 1000 predictions. The performance of the proxy and prey models were  
270 evaluated by comparing the percentage deviance explained and the predictive maps derived  
271 from the final models.

### 272 **3. RESULTS**

273 Sightings and effort data from 292 dedicated cetacean surveys were available to investigate  
274 temporal and spatial patterns in fin whale habitat use in the JCP. In total, 1878 hours were  
275 spent on effort, of which 510 hours were characterised as handling time during which the  
276 researchers were collecting photo-ID or biopsy data, leaving 1368 hours of corrected effort  
277 (Table 2, Fig. 2). Overall, 2986 individual fin whales were recorded on effort, with an average  
278 group size of 2.19 animals (SE = 0.05). Average annual encounter rates and median group  
279 sizes decreased over the study period (Table 2).

#### 280 *3.1. Proxy-fin whale distribution models*

281 Out of the five models fitted with proxy variables, the model which included an interaction  
282 term of aspect and month performed best in terms of AIC, percentage deviance explained  
283 and ASPE (Table 3). Distance to coast, Chl  $a$ , spring Chl  $a$ , spring SST, NAO index, and lagged  
284 winter NAO indices were shrunk to zero degrees of freedom by the shrinkage regression  
285 splines and simultaneously dropped from the model (Model 1.3 Table 3). Winter NAO index  
286 was subsequently dropped from the model, because it was the only term with an  
287 approximate  $P$ -value  $> 0.05$  and very low effective degrees of freedom (edf = 0.19). The  
288 resulting final proxy model explained 24.2 % of deviance.

289 Among the covariates retained in the final model, water depth and aspect were of the  
290 highest importance, with fin whales occurring in greater numbers in deeper waters, over

291 steep, and northward facing slopes (Fig. 3). Higher numbers were also recorded at SST  
292 greater than 12°C. Temporal trends suggested a peak in fin whales at the onset of the survey  
293 season in June, followed by a decline until September, and a second peak at the end of the  
294 season in October. The affinity to northward facing slopes changed by month, showing that  
295 occurrence at southward facing slopes was less likely in August and September, compared to  
296 June, July and October. The negative yearly trend that was already reported for the annual  
297 fin whale encounter rates was also reflected in the final model.

### 298 *3.2. Prey- fin whale distribution models*

299 The prey model that included an interaction term between krill biomass and month had the  
300 lowest ASPE and AIC score and highest percentage of deviance explained (11.8 %) among all  
301 three built models (Table 3). Krill biomass had the highest importance among the model  
302 covariates, followed by month and year. The intra- (month) and inter-seasonal (year)  
303 patterns followed the same trends as described for the proxy model (Fig. 4). Fin whale  
304 numbers increased with higher modelled krill biomass, although the interaction term  
305 indicated that fin whales also occurred in areas with lower krill biomass at the onset of the  
306 season (June and July).

### 307 *3.3. Prediction*

308 Annual predictive maps of average fin whale occurrence generated from the final proxy and  
309 prey fin whale models are shown in Figs. 5 & 6, with CV in Supplement 4 (Figs. S6 & S7).  
310 From the proxy model, two main areas with consistently high predicted relative abundance  
311 of fin whales were identified: the western end of the Anticosti Channel and the area north of  
312 Banc Parent (see Fig. 1 for locations). The area off Banc Parent coincides with the southern  
313 branching traffic shipping lanes. The predictive maps indicated a potential third high density

314 area on the northern edge of the Laurentian Channel. However, this area of very high  
315 predicted relative abundance lies at the very southwestern edge of our survey area and  
316 could represent an “edge effect” because the area is the deepest in the surveyed area with  
317 little effort extending that far. A clear annual decline in fin whale numbers was evident from  
318 the predictive maps.

319 Predictions from the prey model favoured a more even spatial distribution of fin whales  
320 across the JCP. The head of the Anticosti Channel to the east and the southwestern area of  
321 the study area seemed to have overall the highest predicted numbers, but the strong signal  
322 of the annual negative trend masked areas with consistently high numbers.

#### 323 **4. DISCUSSION**

324 SDMs were fitted to understand the extent to which the observed decline in fin whale  
325 numbers was a result of changing environmental conditions in the northern GSL . The proxy  
326 and prey models both identified the negative annual trend in the number of fin whale  
327 individuals, but the proxy model had overall a better predictive performance than the prey  
328 model. Here, we discuss the link between the observed decline in fin whales and the spatio-  
329 temporal patterns that were revealed by the SDMs.

330 Over the study period, the majority of sightings clustered around the head of the Anticosti  
331 Channel and north of Banc Parent with some inter-annual variability. This distribution was  
332 best reflected in the predictive maps of the proxy model, while the prey model largely failed  
333 to highlight those high density areas. The static bathymetric features in the areas with  
334 consistently high predicted fin whale numbers, characterised by deep water and steep,  
335 northward facing slopes, were the most important predictors in the proxy model. Among all  
336 the dynamic covariates (Chl  $a$ , SST, NAOI), which could explain the inter-annual variability in

337 sightings, only SST was retained in the final proxy model. Fin whale numbers increased in  
338 waters with higher SST, suggesting that cooling of SST could have led to the observed annual  
339 decline. However, a trend analysis showed that the GSL is undergoing warming of SST, with  
340 the northeastern Gulf warming at a faster pace than the southern part of the Gulf (Galbraith  
341 et al. 2012, Larouche & Galbraith 2016). In our study area, both the lowest and highest  
342 average SST in the study area were recorded in 2007 and 2008, respectively, which were also  
343 the years with the highest encounter rates (Fig. S8). Since 2012, near-record temperatures of  
344 both surface and deep layers of the GSL were found to correlate with variations in plankton  
345 phenology and fish abundance (Plourde et al. 2015, Brosset et al. 2018). While results  
346 presented here suggest that a direct correlation between decreasing fin whale abundance  
347 and SST is unlikely, it remains unclear to what extent cascading effects of a warming Gulf  
348 could have impacted fin whale abundance and/or distribution indirectly.

349 The final proxy model explained 24.2 % of the variability in the data, indicating that  
350 important explanatory variables were missing from the model. On a feeding ground, a strong  
351 predator-prey relationship is expected in baleen whales (Piatt et al. 1989, Ressler et al.  
352 2015). No real-time, high-resolution euphausiid data were collected during the cetacean  
353 surveys, so we used modelled krill biomass to test how well it explained fin whale relative  
354 abundance compared to a model using proxy covariates. While the prey model found a  
355 positive relationship between modelled krill biomass and fin whale numbers, the model  
356 performed poorly overall compared to the proxy model in terms of percentage of deviance  
357 explained and predictive power. The modelled krill biomass variable was thus not a suitable  
358 alternative to the proxy variables in this study. The uncertainty associated with the krill  
359 biomass covariate (predicted from a model that explained 24.5% of deviance (Plourde et al.  
360 2016), could have decreased its power as a predictor on a fine spatial scale. This does not

361 preclude a better predictive performance at larger spatial scales. Previous models found  
362 differing relationships between fin whale and euphausiid abundance, possibly due to  
363 differences in spatial scales (Zerbini et al. 2016). Laidre et al. (2010) highlighted the  
364 importance of high spatio-temporal synchrony in the collection of prey and cetacean data to  
365 quantify their relationship. We therefore recommend to explore the performance of  
366 modelled krill biomass as predictor of baleen whale distribution at broader spatial scales in  
367 the GSL.

368 Another factor that could have contributed to the lower performance of the prey model is  
369 the generalist diet of fin whales. While euphausiids are an integral part of their diet, fin  
370 whales are also known to switch prey depending on availability (Gavrilchuk et al. 2014,  
371 Ressler et al. 2015). The inclusion of interaction terms in both models indicated that habitat  
372 use changed as the season progressed. The higher number of fin whales found on southward  
373 facing slopes and at lower krill biomass at the beginning of the season (June-July) coincided  
374 with the rolling of capelin (*Mallotus villosus*) along the North Shore (MPO 2003). To fully  
375 quantify the complex predator-prey relationship in fin whales, we need to gain a better  
376 understanding of their feeding ecology, especially threshold values at which prey switching  
377 occurs, and obtain higher (spatial and temporal) resolution data from all potential prey  
378 species. In the absence of such data, it cannot be excluded that inter-annual variability in  
379 prey availability was, at least partly, the cause of the observed annual decline in fin whale  
380 numbers in the northern GSL.

381 In addition to environmental variability, anthropogenic pressures could affect habitat use  
382 and relative abundance. The high density area identified north of Banc Parent coincided with  
383 the southern branch of the shipping lanes. In fact, more than a fifth (22.6 %) of all fin whale  
384 sightings in this study occurred inside the shipping corridor, posing a considerable risk of ship

385 collisions and noise pollution. Fin whales are the most commonly reported species in the  
386 current global vessel strike data set maintained by the Scientific Committee of the  
387 International Whaling Commission (Van Waerebeek & Leaper 2008, Van Der Hoop et al.  
388 2013). Based on marine mammal stranding records in the GSL from 1994 to 2008, ship  
389 collision was the most common anthropogenic trauma for fin whales (22%; Truchon et al.  
390 2018). Shipping traffic is projected to increase in the GSL with the opening of the Northwest  
391 Passage (Pizzolato et al. 2016). The predicted areas of high fin whale density described here  
392 should be included in future risk assessments to mitigate the potential impact of shipping on  
393 fin whales (Redfern et al. 2013). Recommended measures could include vessel speed limits  
394 and area avoidance recommendations, which were shown to significantly reduce ship strikes  
395 with North Atlantic right whales (Laist et al. 2014).

396 While the modelling conducted could not provide a clear indication of the cause of the  
397 annual fin whale decline, it did offer valuable insights into spatio-temporal patterns of fin  
398 whale habitat use in the northern GSL. Importantly, the predictions derived from the proxy  
399 model highlighted two key areas with recurrently occurring high fin whale abundance. The  
400 bathymetric features which characterise those areas were in line with previous findings,  
401 which have also found water depth and slope to be important predictors of fin whale  
402 occurrence in the Mediterranean Sea (Panigada et al. 2005, Azzellino et al. 2012, Pennino et  
403 al. 2016), in the northeastern Atlantic (Víkingsson et al. 2015), and the Bay of Fundy  
404 (Woodley & Gaskin 1996, Ingram et al. 2007). Krill and capelin aggregate along shelf breaks  
405 and steep slopes as a result of tidal currents and upwelling in the GSL and St. Lawrence  
406 Estuary (Simard et al. 2002, Cotté & Simard 2005). The two high fin whale density areas  
407 coincide with the two areas of above average krill biomass accumulation identified in the JCP  
408 by large-scale hydroacoustic surveys (McQuinn et al. 2015). A potential third high density

409 area was predicted along the northern slopes of the Laurentian Channel, which received  
410 little survey effort during this study. This predicted high density area could be an edge effect  
411 (i.e. an artefact); future surveys of this area are needed to identify whether or not this area  
412 is important habitat for fin whales.

413 This study has shown how data collected on surveys primarily designed for other purposes  
414 can be adapted for habitat modelling analysis. However, this *ad hoc* adaptation of the data  
415 leads to a number of concessions. In the absence of distance-sampling and a design ensuring  
416 equal coverage probability, it was not possible to estimate absolute density or abundance  
417 throughout the study area using design-based methods. While the model-based approach  
418 used here accounted for uneven distribution of effort through the inclusion of an offset  
419 term, we were able to describe only relative variability in abundance and distribution. The  
420 focus on sampling individuals rather than space further compromised search effort data.  
421 Such a disruption of search effort could lead to bias in the effort quantification and the  
422 inclusion of duplicate sightings, when previously encountered animals catch up with the  
423 survey boat. The particular setup of this study allowed us to identify duplicate sightings from  
424 the photo-identification data and to correct for handling time based on detailed field notes.  
425 Without standardised sampling design, data from opportunistic platforms generally require  
426 data-specific solutions. However, the data described here share many similarities with data  
427 collected from other platforms of opportunity, such as whale watching boats. We therefore  
428 propose that the correction of effort for handling time is applicable to other data sets  
429 compromised by disrupted search effort, and its application could allow hitherto unused  
430 data to provide useful information on distribution and habitat use.

431

432 **Acknowledgments**

433 We thank the sponsors and supporters of the Mingan Island Cetacean Study (MICS) and its  
 434 numerous volunteers, team members, and captains for data collection and handling over all  
 435 these years. A. Schleimer was supported by the Luxembourg National Research Fund (FNR;  
 436 AFR/11256673) and Odyssea. We are also grateful to three anonymous reviewers for  
 437 constructive comments on the manuscript.

438 **Literature Cited**

- 439 Akaike H (1972) Information theory and an extension of the maximum likelihood principle.  
 440 Proc 2nd Int Symp Inf Theory, Supp to Probl Control Inf Theory:267–281
- 441 Azzellino A, Panigada S, Lanfredi C, Zanardelli M, Airoidi S, Notarbartolo di Sciara G (2012)  
 442 Predictive habitat models for managing marine areas: Spatial and temporal distribution  
 443 of marine mammals within the Pelagos Sanctuary (Northwestern Mediterranean Sea).  
 444 Ocean Coast Manag 67:63–74
- 445 Becker EA, Forney KA, Fiedler PC, Barlow J, Chivers SJ, Edwards CA, Moore AM, Redfern JV  
 446 (2016) Moving towards dynamic ocean management: How well do modeled ocean  
 447 products predict species distributions? Remote Sens 8:1–26
- 448 Bourque MC, Kelley DE, Bourque M, Kelley DE (1995) Evidence of wind-driven upwelling in  
 449 Jacques-Cartier Strait. Atmosphere-Ocean 33:621–637
- 450 Brosset P, Doniol-Valcroze T, Swain DP, Lehoux C, Beveren E Van, Mbaye BC, Emond K,  
 451 Plourde S (2018) Environmental variability controls recruitment but with different  
 452 drivers among spawning components in Gulf of St. Lawrence herring stocks. Fish  
 453 Oceanogr 28:1–17
- 454 Bui AOV, Ouellet P, Castonguay M, Brêthes JC (2010) Ichthyoplankton community structure  
 455 in the northwest Gulf of St. Lawrence (Canada): Past and present. Mar Ecol Prog Ser  
 456 412:189–205
- 457 Cañadas A, Sagarminaga R, de Stephanis R, Urquiola E, Hammond PS (2005) Habitat  
 458 preference modelling as a conservation tool: proposals for marine protected areas for  
 459 cetaceans in southern Spanish waters. Aquat Conserv Mar Freshw Ecosyst 15:495–  
 460 521 Cotté C, Simard Y (2005) Formation of dense krill patches under tidal forcing at  
 461 whale feeding hot spots in the St. Lawrence Estuary. Mar Ecol Prog Ser 288:199–210

- 462 Croll D, Marinovic B, Benson S, Chavez F, Black N, Ternullo R, Tershy B (2005) From wind to  
463 whales: trophic links in a coastal upwelling system. *Mar Ecol Prog Ser* 289:117–130
- 464 Doniol-Valcroze T, Berteaux D, Larouche P, Sears R (2007) Influence of thermal fronts on  
465 habitat selection by four rorqual whale species in the Gulf of St. Lawrence. *Mar Ecol*  
466 *Prog Ser* 335:207–216
- 467 Florko KRN, Bernhardt W, Breiter CJC, Ferguson SH, Hainstock M, Young BG, Petersen SD  
468 (2018) Decreasing sea ice conditions in western Hudson Bay and an increase in  
469 abundance of harbour seals (*Phoca vitulina*) in the Churchill River. *Polar Biol* 41:1187–  
470 1195
- 471 Forney KA, Ferguson M, Becker E, Fiedler P, Redfern JV, Barlow J, Vilchis I, Ballance L (2012)  
472 Habitat-based spatial models of cetacean density in the eastern Pacific Ocean. *Endanger*  
473 *Species Res* 16:113–133
- 474 Fossheim M, Primicerio R, Johannesen E, Ingvaldsen RB, Aschan MM, Dolgov AV (2015)  
475 Recent warming leads to a rapid borealization of fish communities in the Arctic. *Nat*  
476 *Clim Chang* 5:673–677
- 477 Galbraith PS, Larouche P, Chassé J, Petrie B (2012) Sea-surface temperature in relation to air  
478 temperature in the Gulf of St. Lawrence: Interdecadal variability and long term trends.  
479 *Deep Res Part II* 77–80:10–20
- 480 Gavrilchuk K, Lesage V, Ramp C, Sears R, Bérubé M, Bearhop S, Beauplet G (2014) Trophic  
481 niche partitioning among sympatric baleen whale species following the collapse of  
482 groundfish stocks in the Northwest Atlantic. *Mar Ecol Prog Ser* 497:285–301
- 483 Greene CH, Pershing AJ (2000) The response of *Calanus finmarchicus* populations to climate  
484 variability in the Northwest Atlantic: basin-scale forcing associated with the North  
485 Atlantic Oscillation. *ICES J Mar Sci* 57:1536–1544
- 486 Hastie T, Tibshirani R (1990) *Generalized additive models*. Chapman & Hall, London
- 487 Hazen EL, Jorgensen S, Rykaczewski RR, Bograd SJ, Foley DG, Jonsen ID, Shaffer SA., Dunne  
488 JP, Costa DP, Crowder LB, Block BA (2013) Predicted habitat shifts of Pacific top  
489 predators in a changing climate. *Nat Clim Chang* 3:234–238
- 490 Hazen EL, Palacios DM, Forney KA, Howell EA, Becker E, Hoover AL, Irvine L, DeAngelis M,  
491 Bograd SJ, Mate BR, Bailey H (2017) WhaleWatch: a dynamic management tool for  
492 predicting blue whale density in the California Current. *J Appl Ecol* 54:1415–1428
- 493 Hoegh-Guldberg O, Mumby PJ, Hooten AJ, Steneck RS, Greenfield P, Gomez E, Harvell CD,  
494 Sale PF, Edwards AJ, Caldeira K, Knowlton N, Eakin CM, Iglesias-Prieto R, Muthiga N,  
495 Bradbury RH, Dubi A, Hatziolos ME (2007) Coral reefs under rapid climate change and  
496 ocean acidification. *Science* 318:1737–1742

- 497 Hurrell JW, Kushnir Y, Ottersen G (2003) An overview of the North Atlantic Oscillation. *Clim*  
498 *Significance Environ Impact Geophys Monogr* 134:1–35
- 499 Ingram SN, Walshe L, Johnston D, Rogan E (2007) Habitat partitioning and the influence of  
500 benthic topography and oceanography on the distribution of fin and minke whales in  
501 the Bay of Fundy, Canada. *J Mar Biol Assoc UK* 87:149–156
- 502 Isojunno S, Matthiopoulos J, Evans PGH (2012) Harbour porpoise habitat preferences:  
503 Robust spatio-temporal inferences from opportunistic data. *Mar Ecol Prog Ser* 448:155–  
504 170
- 505 Johnston DW, Bowers MT, Friedlaender AS, Lavigne DM (2012) The effects of climate change  
506 on harp seals (*Pagophilus Groenlandicus*). *PLoS ONE* 7:e29158
- 507 Kim YJ, Gu C (2004) Smoothing spline Gaussian regression: More scalable computation via  
508 efficient approximation. *J R Stat Soc Ser B Stat Methodol* 66:337–356
- 509 Laidre K, Heide-Jørgensen M, Heagerty P, Cossio A, Bergström B, Simon M (2010) Spatial  
510 associations between large baleen whales and their prey in West Greenland. *Mar Ecol*  
511 *Prog Ser* 402:269–284
- 512 Laist DW, Knowlton AR, Pendleton D (2014) Effectiveness of mandatory vessel speed limits  
513 for protecting North Atlantic right whales. *Endanger Species Res* 23:133–147
- 514 Larouche P, Galbraith PS (2016) Canadian Coastal Seas and Great Lakes Sea Surface  
515 Temperature Climatology and Recent Trends. *Can J Remote Sens* 42:243–258
- 516 Marra G, Wood SN (2011) Practical variable selection for generalized additive models.  
517 *Comput Stat Data Anal* 55:2372–2387
- 518 McQuinn IH, Plourde S, Pierre JF St., Dion M (2015) Spatial and temporal variations in the  
519 abundance, distribution, and aggregation of krill (*Thysanoessa raschii* and  
520 *Meganyctiphanes norvegica*) in the lower estuary and Gulf of St. Lawrence. *Prog*  
521 *Oceanogr* 131:159–176
- 522 MPO (2003) Capelan de l'estuaire et du golfe du Saint-Laurent (4RST) en 2002. MPO - Sci  
523 *Rapp sur l'état des Stock* 2003/009:1–14
- 524 Panigada S, Notarbartolo di Sciara G, Zanardelli Panigada M, Airoldi S, Borsani JF, Jahoda M  
525 (2005) Fin whales (*Balaenoptera physalus*) summering in the Ligurian Sea: distribution,  
526 encounter rate, mean group size and relation to physiographic variables. *J Cetacean Res*  
527 *Manag* 7:137–145
- 528 Pennino MG, Mérigot B, Fonseca VP, Monni V, Rotta A (2016) Habitat modeling for cetacean  
529 management: Spatial distribution in the southern Pelagos Sanctuary (Mediterranean  
530 Sea). *Deep Res Part II Top Stud Oceanogr* 141:203–211

- 531 Phillips SJ, Dudík M, Elith J, Graham CH, Lehmann A, Leathwick J, Ferrier S (2009) Sample  
532 selection bias and presence-only distribution models: Implications for background and  
533 pseudo-absence data. *Ecol Appl* 19:181–197
- 534 Piatt J, Methven D, Burger A, McLagan R, Mercer V, Creelman E (1989) Baleen whales and  
535 their prey in a coastal environment. *Can J Zool* 67:1523–1530
- 536 Pizzolato L, Howell SEL, Dawson J, Laliberté F, Copland L (2016) The influence of declining sea  
537 ice on shipping activity in the Canadian Arctic. *Geophys Res Lett* 43:12,146–12,154
- 538 Plourde S, Galbraith PS, Lesage V, Grégoire F, Bourdages H, Gosselin J-F, McQuinn I, Scarratt  
539 M (2014) Ecosystem perspective on changes and anomalies in the Gulf of St. Lawrence:  
540 a context in support of the management of the St. Lawrence beluga whale population.  
541 DFO Can Sci Advis Sec Res Doc 2013/129:v + 29p
- 542 Plourde S, Grégoire F, Lehoux C, Galbraith PS, Castonguay M, Ringuette M (2015) Effect of  
543 environmental variability on body condition and recruitment success of Atlantic  
544 Mackerel (*Scomber scombrus* L.) in the Gulf of St. Lawrence. *Fish Oceanogr* 24:347–363
- 545 Plourde S, Lehoux C, McQuinn IH, Lesage V (2016) Describing krill distribution in the western  
546 North Atlantic using statistical habitat models. *Fish Ocean Canada Can Sci Advis Secur*  
547 111:v + 34 p
- 548 QGIS Development Team (2016). QGIS Geographic Information System. Open Source  
549 Geospatial Foundation Project.
- 550 R Core Team. 2015. R: A language and environment for statistical computing. R Foundation  
551 for Statistical Computing, Vienna, Austria. URL <https://www.R-project.org/>.
- 552 Ramp C, Delarue J, Palsbøll PJ, Sears R, Hammond PS (2015) Adapting to a warmer ocean -  
553 Seasonal shift of baleen whale movements over three decades. *PLoS ONE* 10: e0121374
- 554 Redfern JV, Ferguson MC, Becker EA, Hyrenbach KD, Good C, Barlow J, Kaschner K,  
555 Baumgartner MF, Forney KA, Ballance LT, Fauchald P, Halpin P, Hamazaki T, Pershing AJ,  
556 Qian SS, Read A, Reilly S, Torres L, Werner F (2006) Techniques for cetacean – habitat  
557 modeling. *Mar Ecol Prog Ser* 310:271–295
- 558 Redfern J V, McKenna MF, Moore TJ, Calambokidis J, Deangelis ML, Becker EA, Barlow J,  
559 Forney KA, Fiedler PC, Chivers SJ (2013) Assessing the Risk of Ships Striking Large  
560 Whales in Marine Spatial Planning. *Conserv Biol* 27:292–302
- 561 Redfern JV, Moore TJ, Fiedler PC, de Vos A, Brownell RL, Forney KA, Becker EA, Ballance LT  
562 (2017) Predicting cetacean distributions in data-poor marine ecosystems. *Divers Distrib*  
563 23:394–408
- 564 Ressler PH, Dalpadado P, Macaulay GJ, Handegard N (2015) Acoustic surveys of euphausiids  
565 and models of baleen whale distribution in the Barents Sea. *Mar Ecol Prog Ser* 527:13–

566 29

- 567 Sahade R, Lagger C, Torre L, Momo F, Monien P, Schloss I, Barnes DKA, Servetto N, Tarantelli  
568 S, Tatián M, Zamboni N, Abele D (2015) Climate change and glacier retreat drive shifts  
569 in an Antarctic benthic ecosystem. *Sci Adv* 1:e1500050
- 570 Savenkoff C, Castonguay M, Chabot D, Hammill MO, Bourdages H, Morissette L (2007)  
571 Changes in the northern Gulf of St. Lawrence ecosystem estimated by inverse  
572 modelling: Evidence of a fishery-induced regime shift? *Estuar Coast Shelf Sci* 73:711–  
573 724
- 574 Schleimer A, Ramp C, Delarue J, Carpentier A, Bérubé M, Palsbøll PJ, Sears R, Hammond PS  
575 (2019) Decline in abundance and apparent survival rates of fin whales (*Balaenoptera*  
576 *physalus*) in the northern Gulf of St. Lawrence. *Ecol Evol* 9: 4231–4244
- 577 Sigurjónsson J (1988) Operational factors of the Icelandic large whale fishery. *Rep Int Whal*  
578 *Comm* 38:327–333
- 579 Sigurjónsson J, Gunnlaugsson T (2006) Revised catch series and cpue for fin whales taken  
580 from the early modern whaling land stations in Iceland. *Int Whal Comm SC/58/PFI4:1–*  
581 *22*
- 582 Simard Y, Lavoie D, Saucier FJ (2002) Channel head dynamics: capelin (*Mallotus villosus*)  
583 aggregation in the tidally driven upwelling system of the Saguenay - St. Lawrence  
584 Marine Park's whale feeding ground. *Can J Fish Aquat Sci* 59:197–210
- 585 Thibodeau B, de Vernal A, Hillaire-Marcel C, Mucci A (2010) Twentieth century warming in  
586 deep waters of the Gulf of St. Lawrence: A unique feature of the last millennium.  
587 *Geophys Res Lett* 37:1–5
- 588 Thomson JA, Burkholder DA, Heithaus MR, Fourqurean JW, Fraser MW, Statton J, Kendrick  
589 GA (2015) Extreme temperatures, foundation species, and abrupt ecosystem change:  
590 an example from an iconic seagrass ecosystem. *Glob Chang Biol* 21:1463–1474
- 591 Thuiller W, Lafourcade B, Engler R, Araújo MB (2009) BIOMOD - A platform for ensemble  
592 forecasting of species distributions. *Ecography (Cop)* 32:369–373
- 593 Torres LG, Read AJ, Halpin P (2008) Fine-scale habitat modeling of a top marine predator: do  
594 prey data improve predictive capacity? *Ecol Appl* 18:1702–17
- 595 Truchon M-H, Measures L, Brêthes J-C, Albert É, Michaud R (2018) Influence of  
596 anthropogenic activities on marine mammal strandings in the estuary and northwestern  
597 Gulf of St. Lawrence, Quebec, Canada, 1994-2008. *J Cetacean Res Manag* 18:11–21
- 598 Tylianakis JM, Didham RK, Bascompte J, Wardle DA (2008) Global change and species  
599 interactions in terrestrial ecosystems. *Ecol Lett* 11:1351–1363

- 600 van der Hoop JM, Moore MJ, Barco SG, Cole TVN, Daoust PY, Henry AG, Mcalpine DF,  
601 Mclellan WA, Wimmer T, Solow AR (2013) Assessment of Management to Mitigate  
602 Anthropogenic Effects on Large Whales. *Conserv Biol* 27:121–133
- 603 Van Waerebeek K, Leaper R (2008) Second Report of the IWC Vessel Strike Data  
604 Standardisation Working Group. *Int Whal Comm Sci Comm Doc SC/60/BC5*, Santiago,  
605 Chile.
- 606 Venables, WN, Ripley BD (2002) *Modern Applied Statistics with S*. Fourth Edition. Springer,  
607 New York. ISBN 0-387-95457-0
- 608 Víkingsson GA, Pike DG, Valdimarsson H, Schleimer A, Gunnlaugsson T, Silva T, Elvarsson BÃ,  
609 Mikkelsen B, Øien N, Desportes G, Bogason V, Hammond PS (2015) Distribution,  
610 abundance, and feeding ecology of baleen whales in Icelandic waters: have recent  
611 environmental changes had an effect? *Front Ecol Evol* 3:1–18
- 612 Virgili A, Racine M, Authier M, Monestiez P, Ridoux V (2017) Comparison of habitat models  
613 for scarcely detected species. *Ecol Modell* 346:88–98
- 614 Visser F, Hartman K, Pierce G, Valavanis V, Huisman J (2011) Timing of migratory baleen  
615 whales at the Azores in relation to the North Atlantic spring bloom. *Mar Ecol Prog Ser*  
616 440:267–279
- 617 Warton DI (2005) Many zeros does not mean zero inflation: comparing the goodness-of-fit of  
618 parametric models to multivariate abundance data. *Environmetrics* 16:275–289
- 619 Williams R, Hedley SL, Hammond PS (2006) Modeling distribution and abundance of  
620 Antarctic baleen whales using ships of opportunity. *Ecol Soc* 11:1
- 621 Wood SN (2006) *Generalized additive models: an introduction with R*. Chapman & Hall
- 622 Wood SN, Pya N, Säfken B (2016) Smoothing Parameter and Model Selection for General  
623 Smooth Models. *J Am Stat Assoc* 111:1548–1563
- 624 Wood SN (2017) *Generalized Additive Models: An Introduction with R* (2nd edition).  
625 Chapman and Hall/CRC.
- 626 Woodley TH, Gaskin DE (1996) Environmental characteristics of North Atlantic right and fin  
627 whale habitat in the lower Bay of Fundy, Canada. *Can J Zool* 74:75–84
- 628 Zerbini AN, Friday NA, Palacios DM, Waite JM, Ressler PH, Rone BK, Moore SE, Clapham PJ  
629 (2016) Baleen whale abundance and distribution in relation to environmental variables  
630 and prey density in the Eastern Bering Sea. *Deep Res Part II Top Stud Oceanogr*  
631 134:312–330
- 632 Zuur AF, Ieno EN, Walker N, Saveliev AA, Smith GM (2009) *Mixed Effects Models and*  
633 *Extensions in Ecology with R*. *Stat Biol Heal*:579pp

634 **Tables**

635 Table 1. Candidate explanatory variables for models to predict fin whale relative abundance  
 636 in the Jacques Cartier Passage.

Variable	Description	Resolution
<b>Static variables</b>		
<b>Depth<sup>a</sup></b>	Water depth (metres) at grid cell centre	1 arc-min
<b>Slope<sup>a</sup></b>	Slope of seafloor (degrees) calculated in QGIS from bathymetry	1 arc-min
<b>Aspect<sup>a</sup></b>	Slope orientation (0° to 360°) calculated in QGIS from bathymetry	1 arc-min
<b>DistCoast<sup>a</sup></b>	Distance to nearest coastline (metres)	1 arc-min
<b>Dynamic proxy variables</b>		
<b>SST<sup>b</sup></b>	Monthly average sea surface temperature (°C)	4 km
<b>Spring SST<sup>b</sup></b>	Seasonal composite of average spring (21 March - 21 June) sea surface temperature (°C)	4 km
<b>Chl <math>\alpha^c</math></b>	Log transformed ( $\log(X + 1)$ ) monthly average chlorophyll $\alpha$ concentration ( $\text{mg m}^{-3}$ )	4 km
<b>Spring Chl <math>\alpha^c</math></b>	Log transformed ( $\log(X + 1)$ ) seasonal composite of average spring (21 March - 21 June) chlorophyll $\alpha$ concentration ( $\text{mg m}^{-3}$ )	4 km
<b>NAOI<sup>d</sup></b>	Monthly Hurrell North Atlantic Oscillation (NAO) index	
<b>WinterNAOI<sup>e</sup></b>	Winter NAO index in winter (December to March) preceding sampling season	
<b>WinterNAOlag1<sup>e</sup></b>	Winter NAOI with one-year lag	
<b>WinterNAOlag2<sup>e</sup></b>	Winter NAOI with two-year lag	
<b>Year</b>	Survey year (2007-2013)	
<b>Month</b>	Survey month (June-October)	
<b>Dynamic prey variables</b>		
<b>Krill biomass<sup>f</sup></b>	Log transformed ( $\log(X + 1)$ ) modelled monthly krill biomass ( $\text{g m}^{-2}$ )	5 km

637 Sources:

638 <sup>a</sup> ETOPO1 1 Arc-Minute Global Relief Model

639 <sup>b</sup> Aqua-MODIS Level-3 sea surface temperature (4 $\mu$  nighttime). DOI  
 640 10.5067/AQUA/MODIS/L3M/SST/2014

641 <sup>c</sup> Aqua-MODIS Level-3 chlorophyll concentration (OCx algorithm). DOI  
 642 10.5067/AQUA/MODIS/L3M/CHL/2018

643 <sup>d</sup> Climate Analysis Section, NCAR, Boulder, USA, Hurrell (2003) accessed 25 May 2017<sup>e</sup> National  
 644 Center for Atmospheric Research Staff (Eds). The Climate Data Guide: Hurrell North Atlantic  
 645 Oscillation (NAO) Index (PC-based).

646 <sup>f</sup> Plourde et al. (2016)

647 Table 2. Summary of annual survey effort (in hours) and the number of fin whale sightings  
 648 with information on the median (and maximum) group sizes of the fin whale encounters.

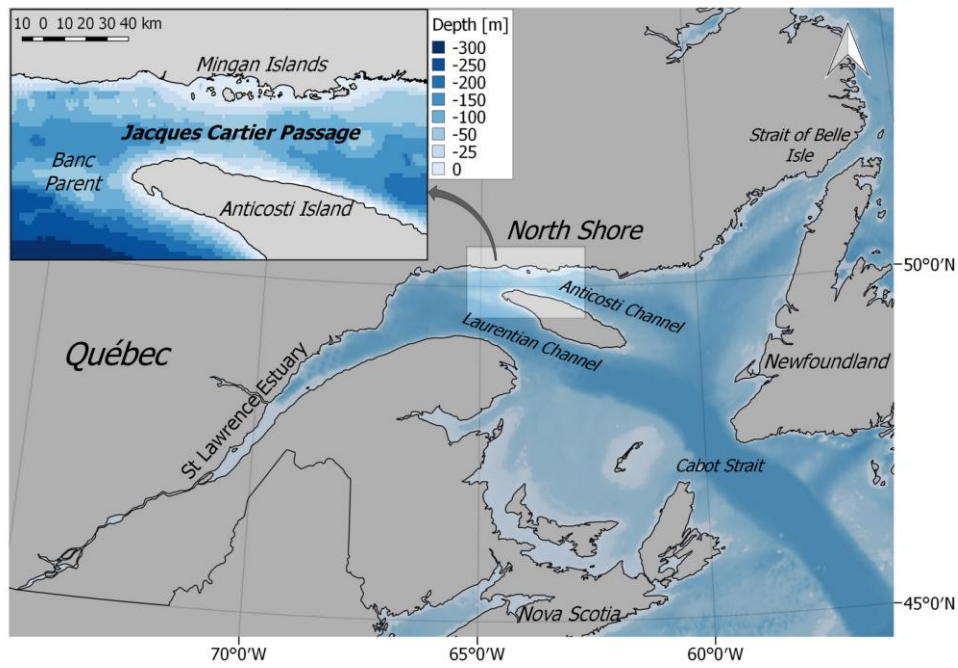
<b>Year</b>	<b>Uncorrected effort</b>	<b>Handling time</b>	<b>Corrected effort</b>	<b>Fin whale sightings</b>	<b>Sightings per corrected hour</b>	<b>Median group size</b>
<b>2007</b>	206.1	37.3	168.8	527	3.12	2 (9)
<b>2008</b>	280.2	81.5	198.7	674	3.39	2 (14)
<b>2009</b>	325.6	112.1	213.5	488	2.29	2 (8)
<b>2010</b>	252.6	70.5	182.1	508	2.79	2 (10)
<b>2011</b>	170.1	59.1	111.0	177	1.60	1 (6)
<b>2012</b>	297.7	89.1	208.6	296	1.42	1 (8)
<b>2013</b>	346.1	60.4	285.7	316	1.11	1 (14)
<b>Total</b>	<b>1878.4</b>	<b>510.0</b>	<b>1368.4</b>	<b>2986</b>		

649 Table 3. Model selection of proxy- and prey-fin whale models with and without interaction  
 650 terms.

Variables	$\theta$	REML	AIC	%Dev	$r^2$	ASPE
<b>1. Proxy Model</b>						
<b>1.1 Penalised Model*</b>	0.17	1068.7	2963.4	20.6	0.38	29.59
<b>1.2 Penalised Model +ti(Depth,month)</b>	0.18	1067.5	2953.4	23.1	0.36	28.83
<b>1.3 Penalised Model +ti(Depth,year)</b>	0.17	1068.5	2963.1	21.1	0.39	27.72
<b>1.4 Penalised Model +ti(Aspect,month)</b>	<b>0.18</b>	<b>1065.0</b>	<b>2944.4</b>	<b>23.7</b>	<b>0.43</b>	<b>25.72</b>
<b>1.5 Penalised Model +ti(Aspect:year)</b>	0.17	1068.4	2961.9	21.5	0.37	28.50
<b>2. Prey Model</b>						
<b>2.1 s(krill) +s(month) +s(year)</b>	0.12	1143.6	3185.2	7.6	0.21	34.29
<b>2.2 s(krill) +s(month) +s(year) +ti(krill,month)</b>	<b>0.13</b>	<b>1138.3</b>	<b>3161.8</b>	<b>11.8</b>	<b>0.23</b>	<b>33.07</b>
<b>2.3 s(krill) +s(month) +s(year) +ti(krill,year)</b>	0.12	1143.2	3184.0	8.1	0.21	34.03

651 \*Full penalised model includes all variables described in Table 1, except for krill biomass:  
 652 s(Depth)+ s(Slope)+ s(Aspect)+ s(DistCoast)+ s(SST)+ s(SpringSST)+ s(Chla)+ s(SpringChla)+  
 653 s(NAOI)+ s(WinterNAOI)+ s(WinterNAOIlag1)+ s(WinterNAOIlag2)+ s(year)+ s(month) with  
 654 automated variable selection using shrinkage smoothers. Model selection was based on  
 655 Akaike Information Criterion (AIC), percentage of deviance explained (%Dev), and mean  
 656 average squared prediction error (ASPE) from a five-fold cross-validation.  $\theta$  = theta  
 657 parameter from negative binomial  $nb()$  error distribution; REML = restricted maximum  
 658 likelihood. Selected models are shown in bold.

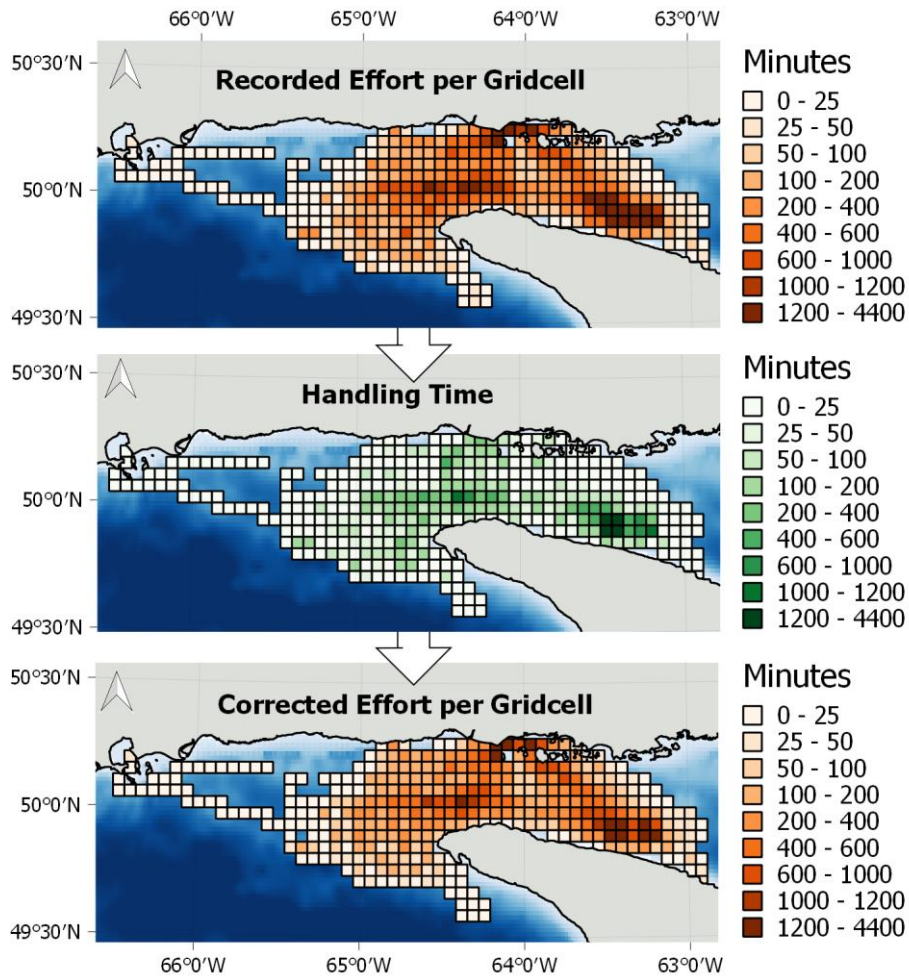
Figures



659

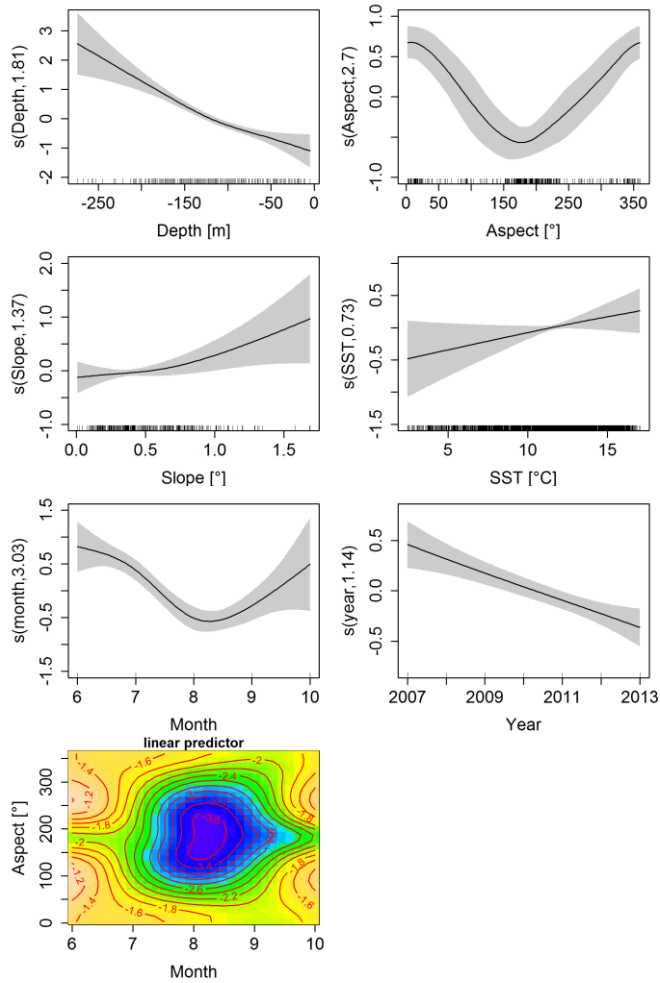
660 Fig. 1. Schematic representation of the Gulf of St. Lawrence, with detailed bathymetry of the  
 661 study area in the Jacques Cartier Passage.

662



663

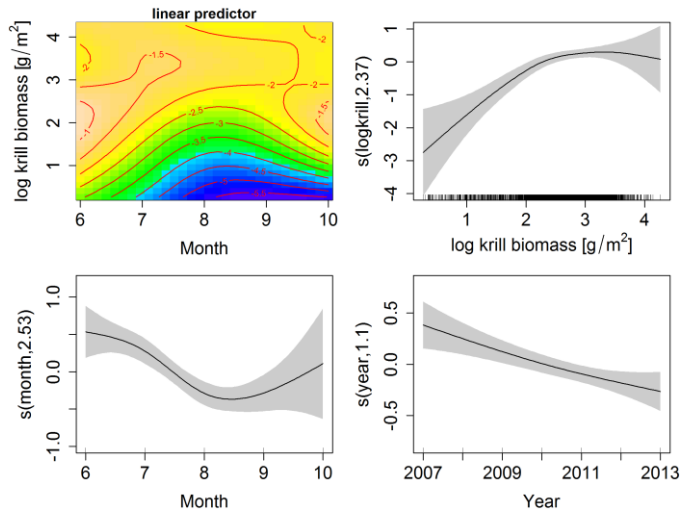
664 Fig. 2. Distribution of total survey effort in the Jacques Cartier Passage in minutes per 25 km<sup>2</sup>  
 665 grid cell over the seven survey years (June to October, 2007 to 2013), followed by the  
 666 amount of handling time and the derived corrected effort per grid cell.



667

668 Fig. 3. Smooth functions fitted in the final proxy-fin whale model. Positive values of the  
 669 smoothed function indicate a positive effect on the response variable. Tick marks on the  
 670 horizontal axis show the distribution of observations, while the smoother terms with  
 671 estimated degrees of freedom (edf) are shown on the vertical axes. Shaded areas represent  
 672 95% confidence intervals. Last plot shows the 2-D interaction between aspect and month  
 673 (5.06 edf, cold colours represent negative effect).

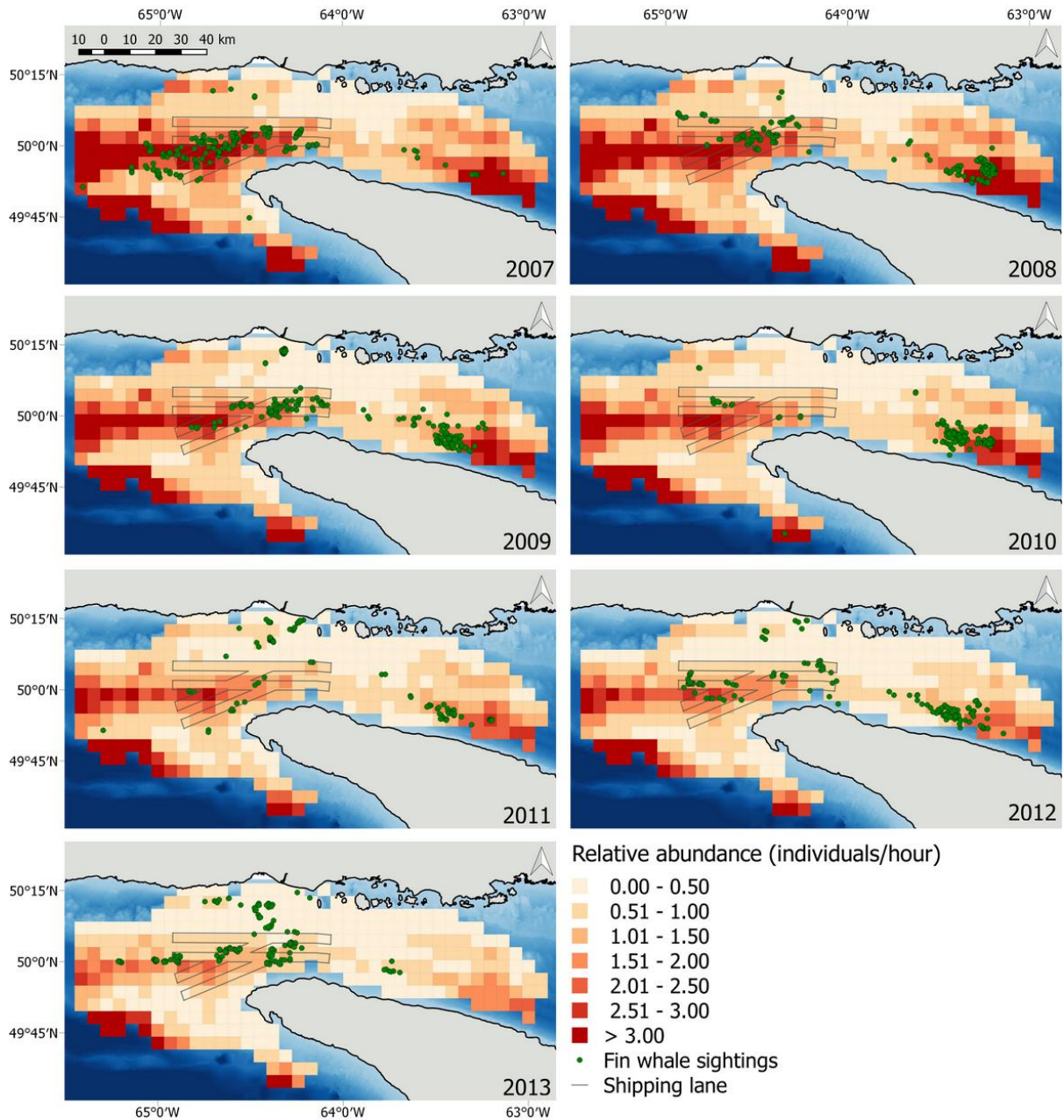
674



675

676

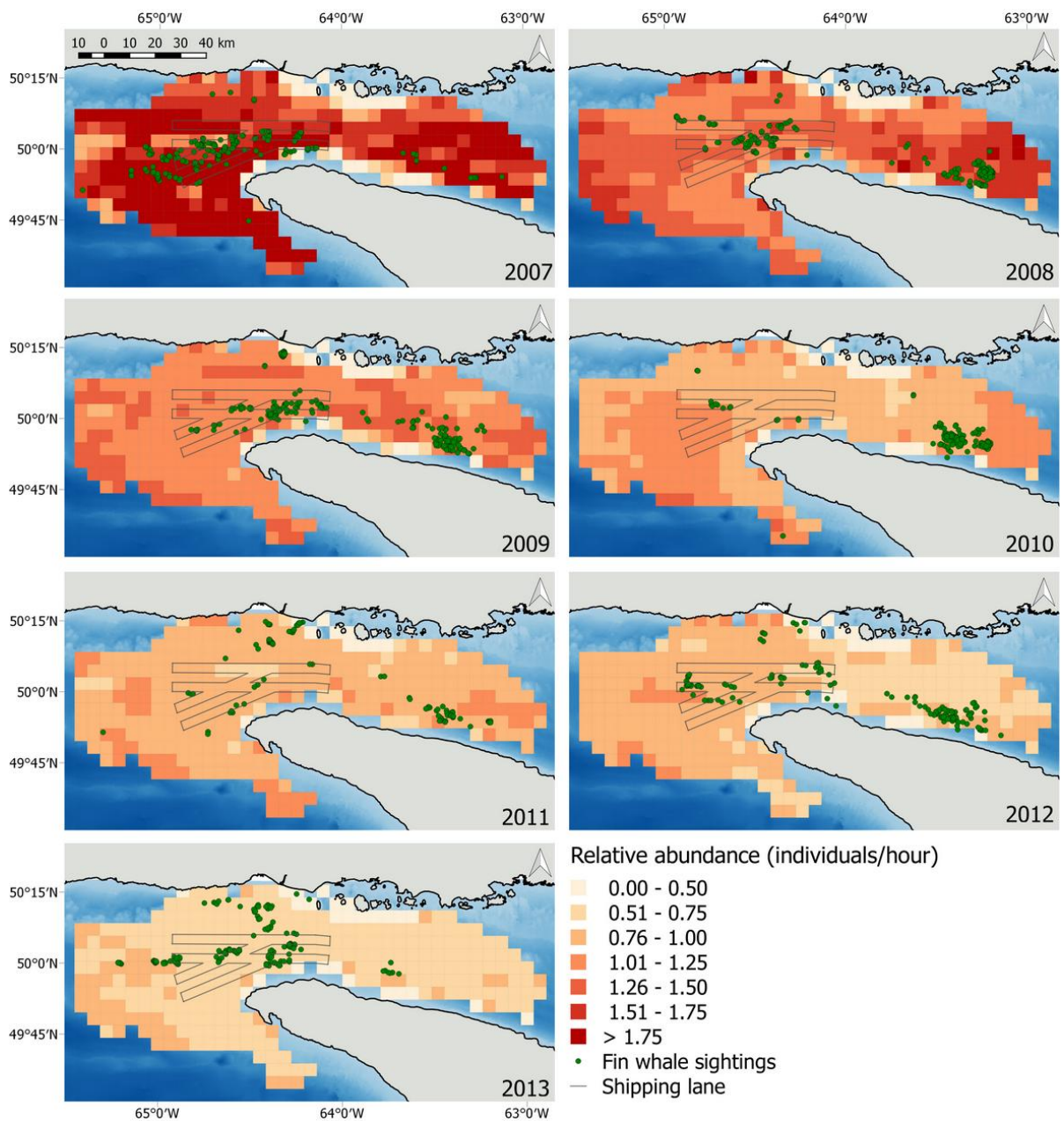
677 Fig. 4. Smooth functions fitted in the final prey-fin whale model. Positive values of the  
 678 smoothed function indicate a positive effect on the response variable. Tick marks on the  
 679 horizontal axis show the distribution of observations, while the smoother terms with  
 680 estimated degrees of freedom (edf) are shown on the vertical axes. Shaded areas represent  
 681 95% confidence intervals. First plot shows the 2-D interaction between krill biomass and  
 682 month (4.63 edf).



683

684 Fig. 5. Predictive maps of relative annual fin whale abundance (individuals per hour effort)  
 685 from the proxy fin whale model. Each map shows the average annual relative abundance of  
 686 fin whales in each grid cell. The dots show the reported sightings of fin whale groups made  
 687 during the surveys in that year.

688



690 Fig. 6. Predictive maps of relative annual fin whale abundance (individuals per hour effort)  
 691 from the prey fin whale model. Each map shows the average annual relative abundance of  
 692 fin whales in each grid cell. The dots show the reported sightings of fin whale groups made  
 693 during the surveys in that year.

694

695

696

697

698

## SUPPORTING INFORMATION

---

699

### **Spatio-temporal patterns in fin whale (*Balaenoptera physalus*) habitat use in the northern Gulf of St. Lawrence**

700

701 Anna Schleimer<sup>1,2,3,\*</sup>, Christian Ramp<sup>1,2</sup>, Stéphane Plourde<sup>4</sup>, Caroline Lehoux<sup>4</sup>, Richard  
702 Sears<sup>2</sup>, Philip S. Hammond<sup>1</sup>

703 <sup>1</sup>Sea Mammal Research Unit, Gatty Marine Laboratory, University of St Andrews, St  
704 Andrews, KY16 8LB UK

705

706 <sup>2</sup>Mingan Island Cetacean Study, St Lambert, Québec, J4P 1T3, Canada

707

708 <sup>3</sup>Marine Evolution and Conservation, Centre for Ecological and Evolutionary Studies,  
709 University of Groningen, Groningen, 9700 CC, The Netherlands

710

711 <sup>4</sup>Institut Maurice-Lamontagne, Fisheries and Oceans Canada, Mont-Joli, Québec, G5H 3Z4,  
712 Canada

713

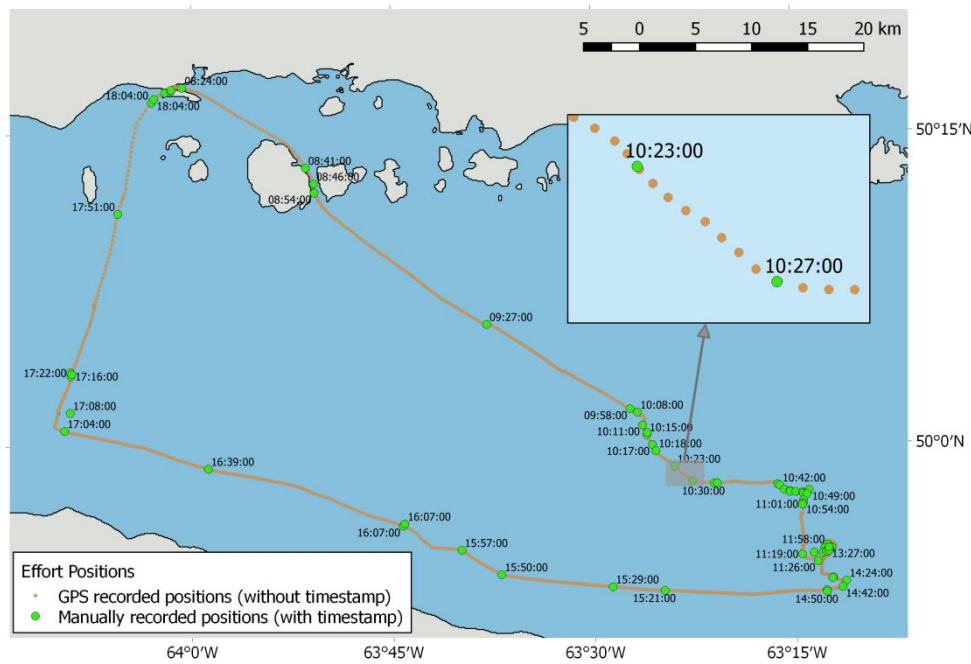
714 **\*Corresponding author:** Anna Schleimer, schleimer.anna@gmail.com

715

#### 716 **Supplement 1**

##### 717 *Effort Calculation*

718 The GPS unit had different sampling settings, including sampling locations at a set temporal  
719 interval and an automatic mode, during which positions were recorded at random time-  
720 interval when the boat was changing direction. However, the GPS units on the boats only  
721 recorded positions in latitude and longitude, without timestamp. Because time was identified  
722 as the most appropriate measure of effort for this study, the first step consisted in associating  
723 timestamps to the GPS locations for the calculation of effort. During the survey, precise  
724 timestamps and positions were recorded manually for events such as survey start, survey stop,  
725 sightings and changes in survey conditions. For each survey track, these recorded timestamps  
726 were associated to the nearest point of the survey track collected on the same day and boat  
727 (Fig. S1). Associations that were made with positions farther than 100m apart were discarded.  
728 Once these timestamps from the survey data were associated to the survey track, the sampling  
729 interval could be estimated by dividing the time difference between two timestamps by the  
730 number of positions recorded by the GPS unit. Depending on the setting, the GPS unit  
731 recorded positions at a 5, 10, or 30 second interval. On an unknown number of surveys the  
732 GPS unit ran on the default automatic mode. For those days it was impossible to reconstruct  
733 the timestamp and all associated sighting and effort data were excluded from future analysis.  
734 Once the sampling interval was determined, the timestamps were reconstructed for all  
735 remaining GPS positions. Data from 292 surveys were retained for the habitat modelling.



736

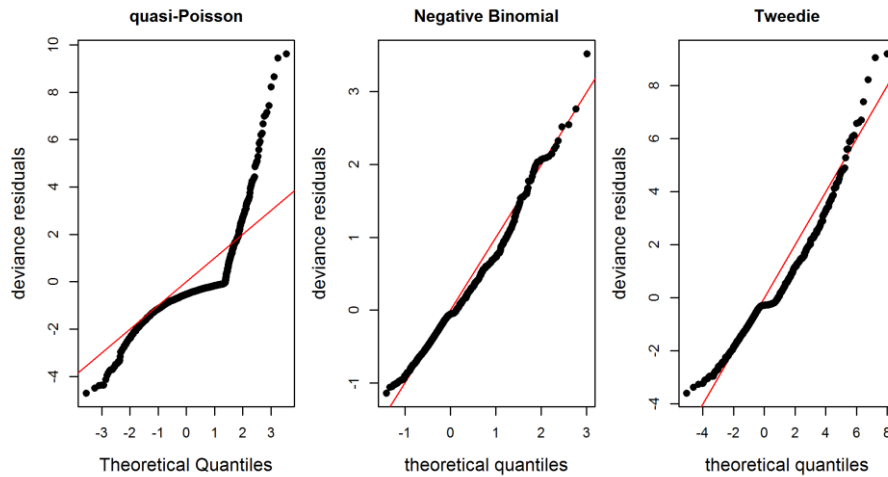
737 Fig. S1. Example of timestamp association procedure from survey on 5 Aug 2008. The time  
 738 interval divided by the number of intermediate GPS positions provides a sampling interval of  
 739 30 sec (=4min/8), allowing the calculation of timestamps for all intermediate GPS location.

740

## 741 Supplement 2

### 742 Error Distribution Selection

743 The response variable was characterised by a high frequency of zeros (3207 grid cells without  
 744 sightings compared to 312 grid cells with sightings), requiring careful choice of the error  
 745 distribution. Quantile-quantile plots were used to compare the performance of three different  
 746 error distributions, namely overdispersed Poisson (quasi-Poisson), negative binomial, and  
 747 Tweedie error distributions for the fin whale occurrence model (Figs S2 & S3). All three error  
 748 structure have been suggested to deal with overdispersed count data and differ mainly by their  
 749 mean-variance relationship (Warton 2005, Ver Hoef & Boveng 2007, Miller et al. 2013).  
 750 Quasi-Poisson and negative binomial share the same number of parameters, but the linear  
 751 mean-variance function of the Quasi-Poisson distribution puts more weight on large counts  
 752 while small counts are more heavily weighted in the negative binomial distribution due to its  
 753 quadratic mean-variance function (Ver Hoef & Boveng 2007). In addition to the mean ( $\mu$ ) and  
 754 dispersion ( $\emptyset$ ) parameters, the Tweedie distribution has a third power ( $p$ ) parameter, offering  
 755 additional flexibility to model count data (Miller et al. 2013). The Tweedie mean-variance  
 756 relationship is described as  $var(Y) = \emptyset\mu^p$  (Miller et al. 2013). Setting  $p$  to 1 gives a quasi-  
 757 Poisson distribution.



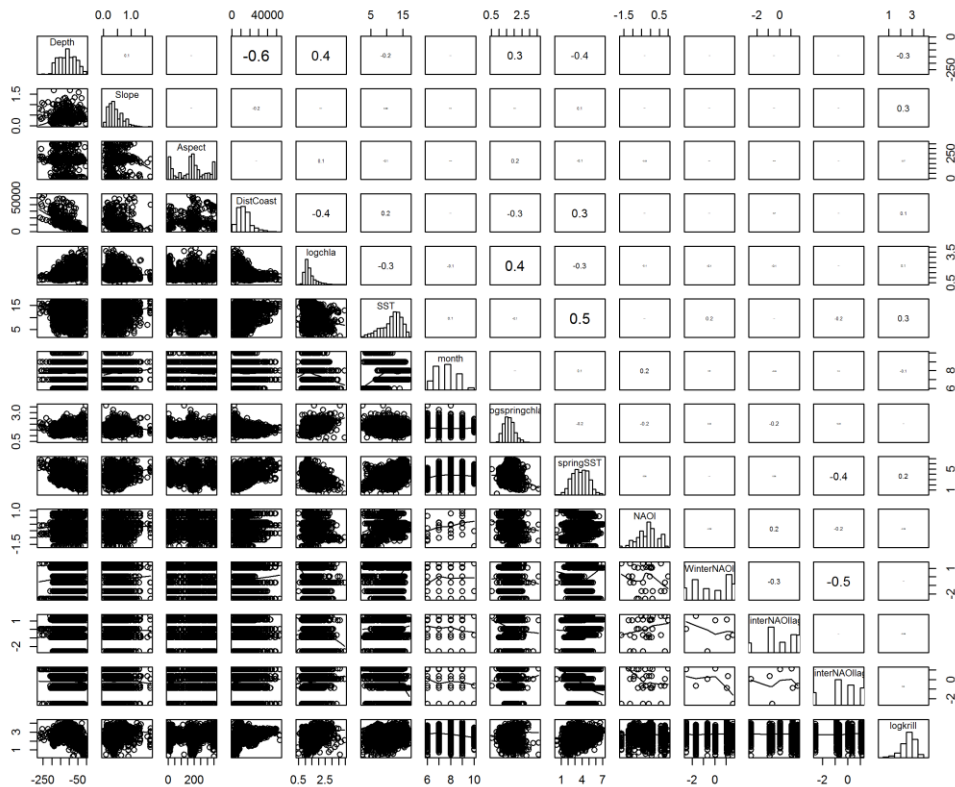
758

759 Fig. S2. Quantile-Quantile plots of proxy model with three different error distributions. The  
760 negative binomial error distribution provided the best fit.

761 **Supplement 3**

762 *Model validation*

763 Collinearity between candidate explanatory was evaluated using the pairs() function in the  
764 AED package. Based on the 0.6 cut-off value, there was no evidence for significant  
765 collinearity that required further investigation (Fig. S3).

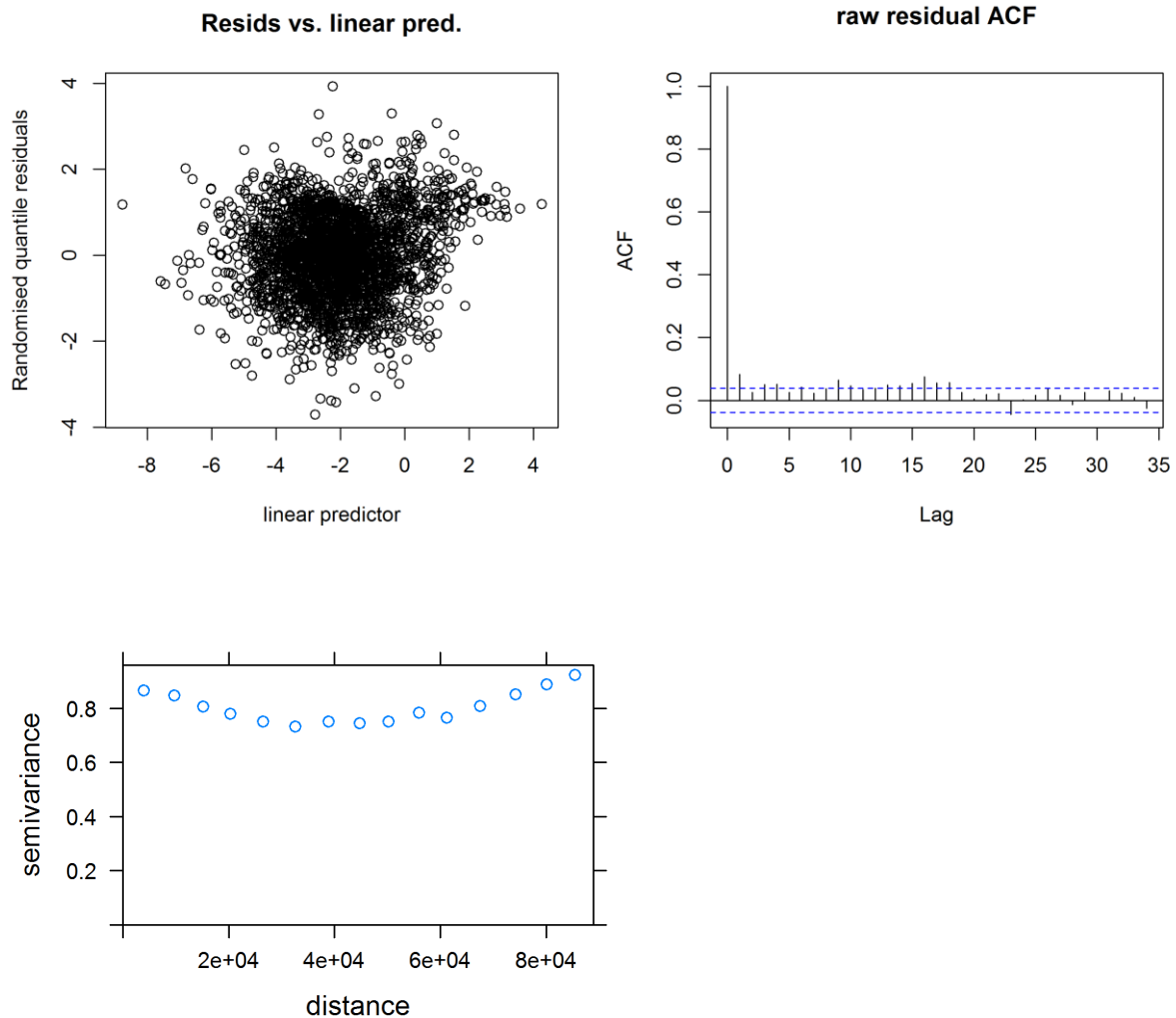


766

767 Fig. S3. Pairplot of candidate explanatory variables, with the upper panel showing estimated  
768 pair-wise correlation coefficients. R-code based on Zuur et al. (2009).

769  
770  
771  
772  
773

Residual plots were investigated to assess assumptions of variance homogeneity and independent errors. There was no indication for variance heterogeneity or autocorrelation for the proxy-fin whale model (Fig. S4) but some indication of autocorrelation in the prey-fin whale model (Fig. S5).

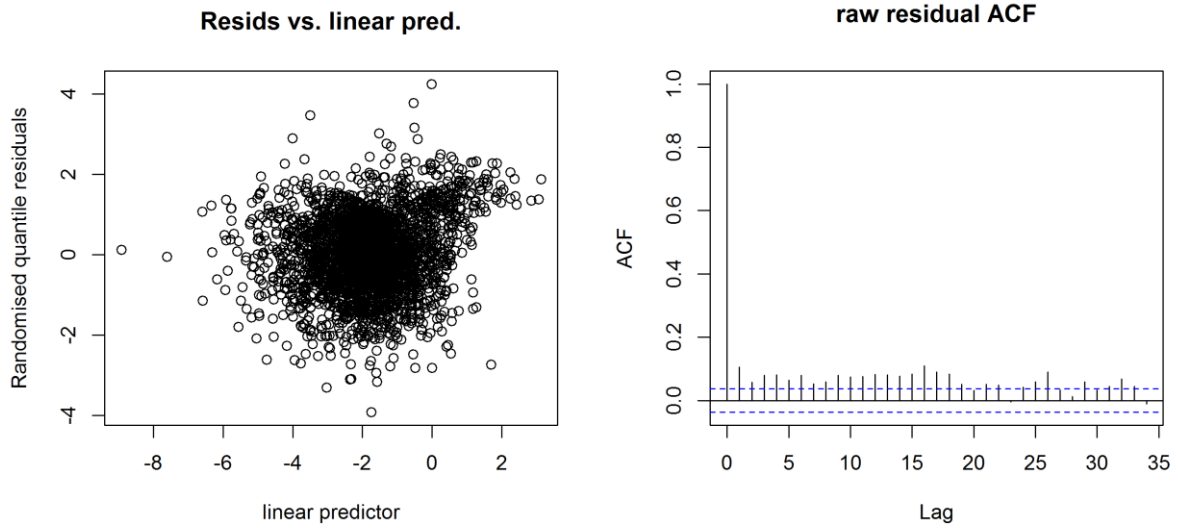


774

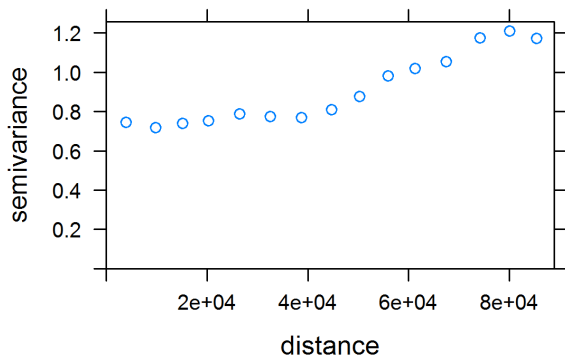
775

776 Fig. S4. Diagnostic residual plot for proxy-fin whale occurrence model. The horizontal band  
777 on the semi-variogram of residuals, with distance on the x-axis and semi-variance on the y-  
778 axis, indicates spatial independence (Zuur et al. 2009).

779



780



781

782 Fig. S5. Diagnostic residual plot for prey-fin whale occurrence model. The horizontal band on  
 783 the semi-variogram of residuals, with distance on the x-axis and semi-variance on the y-axis,  
 784 indicates spatial independence (Zuur et al. 2009).

785

786

787

788

789

790

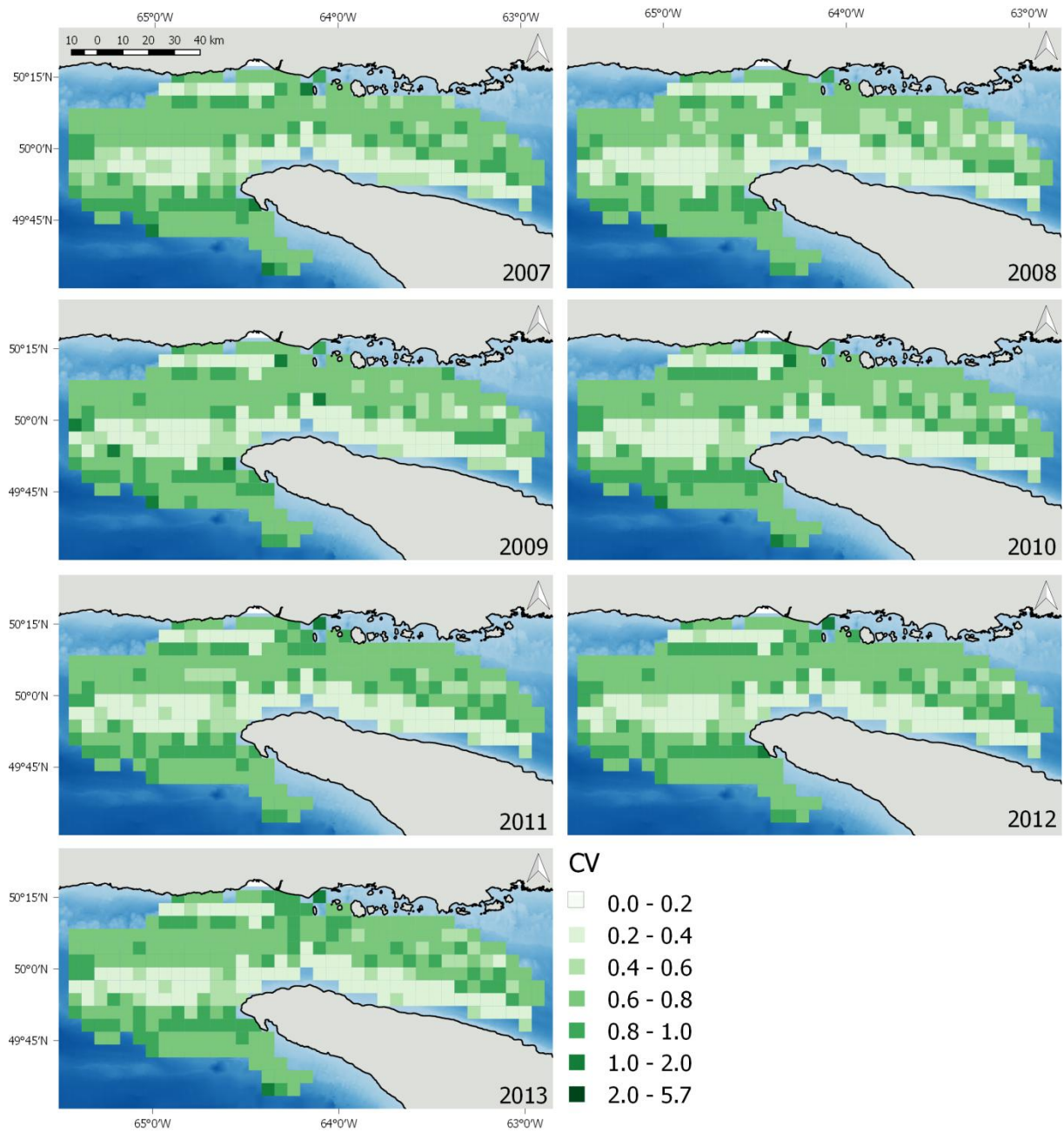
791

792

793

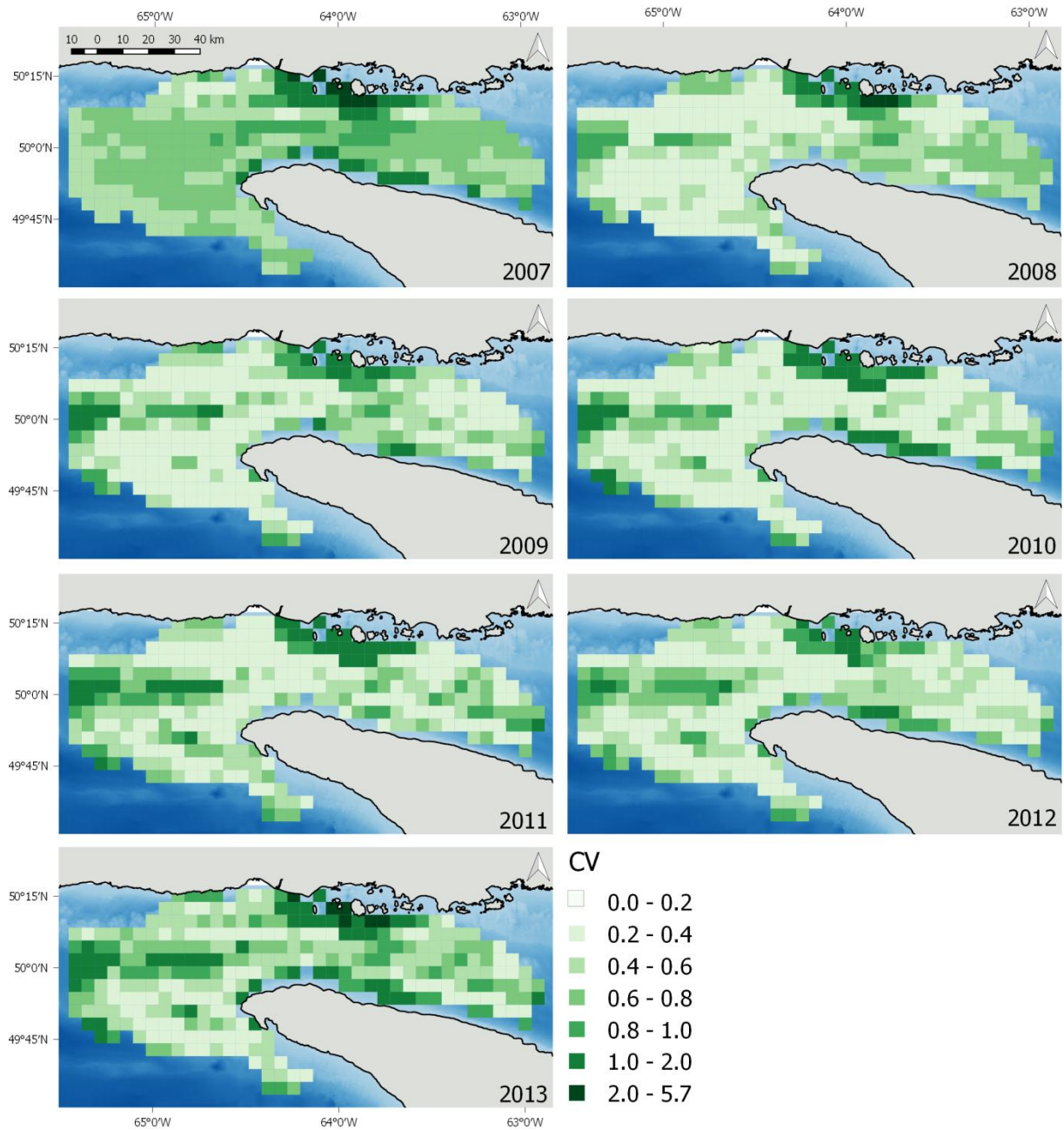
794 **Supplement 4**

795 *Uncertainty distribution of model predictions*



796

797 Fig. S6. Coefficients of variation (CV) of annual average predictions from the proxy-fin  
798 whale model.



799

800 Fig. S7. Coefficients of variation (CV) of annual average predictions from the prey-fin whale  
801 model.

802

803

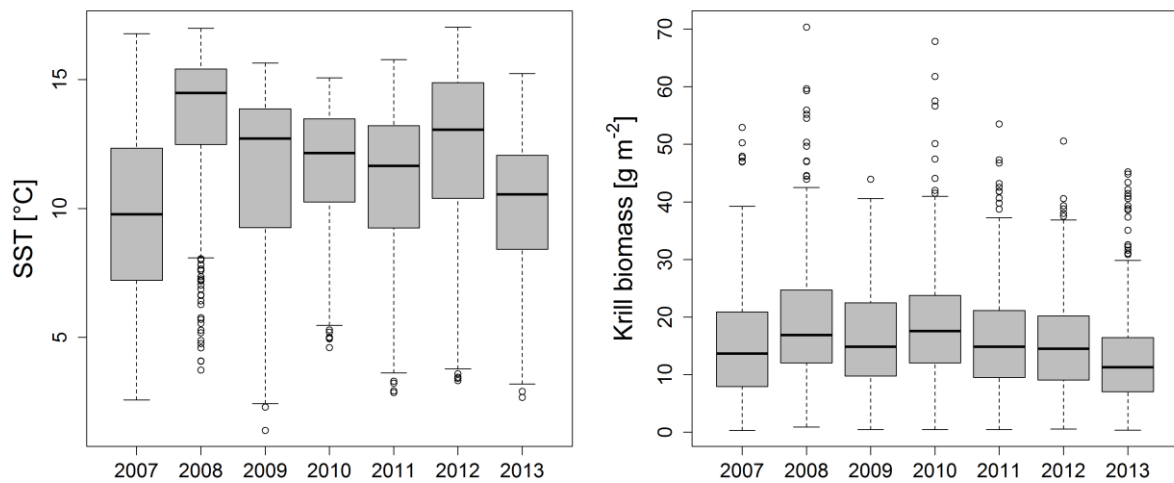
804

805

806

807

808

809 **Supplement 5**810 *Summary of annual trends*

811

812 Fig. S8. Average annual sea surface temperatures (SST) and modelled krill biomass over all  
 813 grid cells.

814 **References**

- 815 Miller DL, Burt ML, Rexstad EA, Thomas L (2013) Spatial models for distance sampling  
 816 data: recent developments and future directions (O Gimenez, Ed.). *Methods Ecol Evol*  
 817 4:1001–1010
- 818 Ver Hoef J, Boveng P (2007) Quasi-Poisson vs. negative binomial regression: how should we  
 819 model overdispersed count data? *Ecology* 88:2766–2772
- 820 Warton DI (2005) Many zeros does not mean zero inflation: comparing the goodness-of-fit of  
 821 parametric models to multivariate abundance data. *Environmetrics* 16:275–289
- 822 Zuur AF, Ieno EN, Walker N, Saveliev AA, Smith GM (2009) *Mixed Effects Models and*  
 823 *Extensions in Ecology with R*. Stat Biol Heal:579pp

824

825